Compressibility of random walker trajectories on growing networks

Robert J. H. Ross,* Charlotte Strandkvist,† and Walter Fontana‡
Department of Systems Biology
Harvard Medical School
200 Longwood Avenue, Boston MA 02115

We find that the simple coupling of network growth to the position of a random walker on the network generates a traveling wave in the frequency distribution of nodes visited by the walker. This suggests that the growth of a space by virtue of a process situated in it constrains its dynamics to a set of typical trajectories. We present arguments that such compressibility indeed holds for our network growth model for all walker motility rates. This property is of interest because although the network size tends to infinity, the uncertainty associated with the walker's position on the network grows no faster than if it were on a non-growing, finite-sized network.

Numerous physical, biological, cognitive, and social processes are situated in growing spaces. Developmental processes during the embryonic development of an organism are an important example of this, as are communication networks. In many instances, the growth of the space can profoundly affect the dynamics of the processes it hosts, as has been shown both experimentally and theoretically in the case of cell migration and proliferation [1–4]. Conversely, processes can shape global characteristics of the space in which they are embedded by determining where growth occurs. For instance, the ongoing development of the internet is determined by its usage, social networks evolve according to the interactions between the individuals that compose the network, and plasticity in the developing brain is driven by action potentials that shape neuronal architecture [5, 6]. Processes that govern growth are often of a local nature, meaning that they can acquire information only from a small region of space surrounding them. That is, the mechanism of growth does not have access to an all-seeing 'global' perspective.

The question we pursue here is whether the coupling of a process situated inside a growing space, and the growth of that space, can cause the process trajectories to condense into a typical set in the sense of Shannon's source coding theorem. The significance of a typical set is that it vastly reduces the uncertainty of the process outcome. To address this question we use a simple model of a random walker whose position on a network constitutes the attachment point for a new node in a growth event. We show that this coupling suffices for the set of walker trajectories to become compressible, which stands in contrast to three other examples in which network growth is decoupled from the walker's position.

By compressibility we mean that the entropy rate of the random walker trajectory on the network is not divergent [7]. The entropy we consider here is the usual Shannon entropy, $H(X) = -\sum_{i=1}^{n} p_i \log p_i$, where X is a discrete random variable taking values in $\Omega = \{1, 2, \ldots, n\}$ with corresponding probabilities $p_{i\in\Omega}$. Our model is related to an approach by Saramäki [8, 9] used in the context of growing scale-free networks, but is a much simplified version intended to clarify the difference between the walker's "inside" perspective and the global "outside" view of the network grown by the process. We refer to our model as "walker-induced network growth" or WING [10].

In WING, a random walker situated on a network steps from node to node following the edges of the network. At each growth event, one new node is connected with a single edge to the location of the walker. This means that just after addition to the network, new nodes are of degree $k = 1$. We treat the model as a continuous-time Markov chain [11] in which the times of occurrence of a movement event and of a growth event are exponentially distributed with rates r_W and r_N, respectively. There is no limit to the size of the network. In [10] we treated the case of multiple self-excluding walkers, but in the present case we will consider only a single walker.

The number of nodes in the network at time t is denoted with $V(t) \in \mathbb{N}$, and the number of edges with $E(t) \in \mathbb{N}$. $V(t) = N(t) + N_0$, where $N(t)$ is the number of growth events that have occurred up to time t, and N_0 the number of nodes in the seed network. Each node i is uniquely labelled at its creation by the count of growth events that have occurred up to and including its creation. Thus, $i \in \{1, 2, ..., V(t)\}$ with the last node labelled $V(t)$. The degree of a node i is denoted by k_i.

We compare the behavior of WING with three distinct network growth mechanisms in which the walker plays no role in determining the location at which the network grows. Rather, the random walker only serves as a local observer of the network. In "uniformly random" growth (UR), a new node of degree k, chosen uniformly at random from the set $\{1, 2, \ldots, V(t)\}$, forms one edge to each of k nodes randomly picked without replacement from within the current network. In "fully connected" growth (FC), a new node connects to all nodes in the current network, which therefore remains fully connected. In the

* robert_ross@hms.harvard.edu
† charlotte_strandkvist@hms.harvard.edu
‡ walter_fontana@hms.harvard.edu

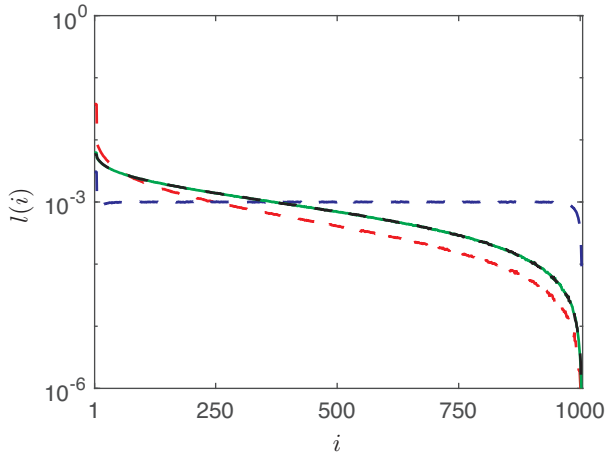

FIG. 1. The frequency of node labels in a trajectory, calculated using (2), depends on the network growth mechanism: WING (blue dashed), BA (red dashed), UR (green dashed), and FC (black dashed). $r_W = 1$, $r_N = 1$, $N = 1000$, averaged over $R = 100,000$ replicates for each growth mechanism.

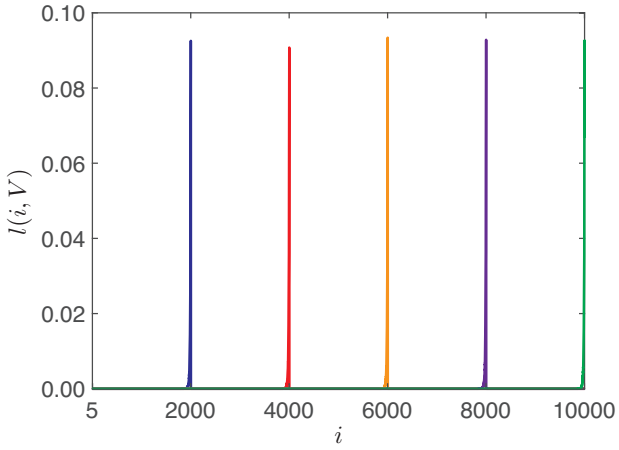

FIG. 2. The graph shows the distribution $l(i, g = V)$ described by (1) recorded at different times or, equivalently, network sizes V. The abscissa is the node label and color indicates the network size ($V = N + N_0$) at which $l(i, V)$ was recorded within the same simulation. $N = 2,000$ (blue), $N = 4,000$ (red), $N = 6,000$ (orange), $N = 8,000$ (purple), and $N = 10,000$ (green). $r_W = 1$, $r_N = 1$, $N_0 = 5$.

Barabási and Albert growth model (BA), at each growth event g, a new node is connected to a single node i in the network with a probability $p_i(g)$ proportional to its degree k_i, $p_i(g) = k_i/[2E(g)]$ with g indexing the growth event. This is also known as preferential attachment. The probability $p_i(g)$ is the same as the equilibrium probability ($r_W \to \infty$) of finding an unbiased random walker at a node of degree k_i in a *non-growing* network. The exact degree distribution generated by the BA model was derived in [12, 13]: $p_{BA}(k) = 4/[k(k+1)(k+2)]$. All these processes hinge on global information about the network in which they are situated, such as the set of all nodes in the network or, in addition, their degree.

Depending on the values of r_W and r_N, WING generates different network structures [8–10, 14]. For instance, if $r_W = 0$, $r_N > 0$, the random walker will not move from its initial position, yielding a network with a 'star' structure. As the ratio $r_W/r_N \to \infty$ in the limit, the probability of finding the walker at node i will become the equilibrium distribution for a non-growing network, thus yielding a network with the BA degree distribution $p_{BA}(k)$. For $0 < r_W < \infty$, and fixed r_N, networks have degree distributions in between these extremes. Importantly, the degree distributions generated by WING with a single walker become rapidly stationary for any fixed values of r_W and r_N [10]. In UR, FC, and BA, the network structure clearly does not depend on the motility of the walker.

To obtain a sense for the behavior of the system, we collect a sample of R trajectories of the random walker. Each trajectory, $\tau_{r,g}$, is a string of node labels, where g indexes the growth event and measures time t. At event g the length of the string is $V(g)$. For example, given the rth trajectory as $\tau_{r,g} = (2, 3, 6, 3, 4, \ldots)$, $\tau_{r,2} = 3$ means that when the second growth event occurred the walker was situated on the node with label 3, which, by assignment of the labels, makes it the third oldest node in the network. The probability of the walker being at node labelled i when the gth growth event happens and the probability of the walker visiting i are respectively:

$$l(i, g) = \frac{1}{R} \sum_{r=1}^{R} \delta(i - \tau_{r,g}), \tag{1}$$

$$l(i) = \frac{1}{V} \sum_{g=1}^{V} l(i, g). \tag{2}$$

where $\delta(x) = 1$ if $x = 0$ and $\delta(x) = 0$ otherwise.

We begin by comparing the numerically obtained label distribution $l(i)$, as described by (2), for UR, FC, BA and WING. Fig. 1 reveals that, for WING, the frequency of any label appearing in a trajectory is essentially uniform. One way of obtaining a uniform distribution is for the random walker to always be at the last node added to the network, which is evidently not random. A uniform distribution is not observed for UR, FC, and BA growth mechanisms. In BA, the age of a node determines its probability of appearing in a trajectory; older nodes appear with higher frequency. The reason for the difference in behavior between UR, FC and BA on the one hand and WING on the other is clear. WING establishes a spatial correlation between the random walker and younger nodes, favoring their inclusion in its trajectory. It is interesting that FC and UR network growth appear to generate the same distribution.

Fig. 2, shows the distribution (1) for WING at progressive times (network sizes), providing some clues. At any given network size V, the mass of the distribution gravitates around the younger nodes. This tendency of the random walker to visit younger nodes in the network

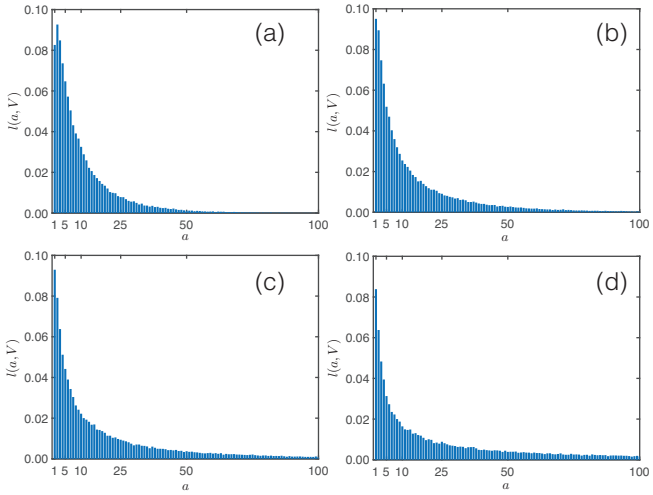

FIG. 3. The distribution $l(a, V)$, where $a = V - i + 1$ is an age label, for different values of r_W plotted against node age. (a): $r_W = 1$; (b): $r_W = 2$; (c): $r_W = 3$; (d): $r_W = 5$. In all panels, $N = 10,000$.

as the network grows, causes a traveling wave in $l(i, V)$.

To examine $l(i, V)$ at different values of the motility r_W, it is more intuitive to relabel nodes with respect to age; thus, a node with growth event label i now becomes a node with age label $a = V - i + 1$, where V is the network size at the time of growth event i. (Age labels of all nodes change with each growth event.) This flips each wave front in Fig. 2 from left to right. Fig. 3 shows that the tail of $l(a, V)$ becomes heavier as r_W is increased. This is to be expected, as increasing r_W relative to r_N counteracts the effect of the spatial correlation between the new node and the random walker. Figures 2 and 3 suggest that the walker's probability of being at a particular node when the next growth event occurs depends on the age of that node and is constant regardless of network size. Figure 3 further suggests this property holds for any fixed r_W and r_N, although the exact values of $l(a, V)$ depend on the ratio of r_W/r_N.

We next study the entropy rates associated with the random walker trajectories. The entropy rate of a stochastic process is defined as

$$H(\mathcal{X}) = \lim_{N\to\infty} \frac{1}{N} H(X_1, X_2, X_3, ..., X_N), \qquad (3)$$

when the limit exists [7]. Given the manner in which we generate $l(i, g)$, it is appropriate to treat each possible random walker trajectory, $(X_1, X_2, X_3, \ldots, X_V)$, as a series of dependent random variables being sampled from a growing probability distribution. Because it is not computationally feasible to obtain this distribution, we treat each X_i as if it were an independent random variable sampled from a growing probability distribution. Assuming independence maximizes the entropy rate associated with repeated sampling from a random variable [7]. We can therefore calculate an upper bound for the entropy

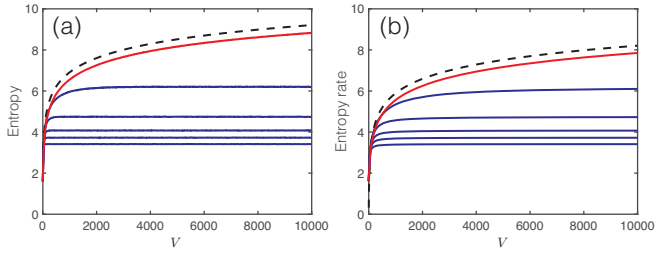

FIG. 4. (a): The Shannon entropy $-\sum_{i=1}^{V} l(i, V) \log l(i, V)$ of $l(i, g = V)$ as defined in (1) is graphed against network size V. (b): The evolution of the bound to the entropy rate, as defined by (4), of $l(i, g = V)$. Growth mechanisms: FC (black dashed), BA (solid red), and WING (solid blue) for different values of r_W. In both panels, the greater r_W, the greater the entropy. Bottom to top: $r_W = 1, 2, 3, 5, 10$.

rate of our trajectories as

$$H(\mathcal{X}) \leq \lim_{N\to\infty} \frac{1}{N} \sum_{n=1}^{N} H(X_n), \qquad (4)$$

where each X_n is a discrete random variable with outcomes in $\{1, 2, \ldots, V\}$. The total number of vertices in the network includes the size, N_0, of the seed network. Thus, X_1 is the first growth event and so has N_0 outcomes, each associated with a probability. Similarly, X_5 is the fifth growth event and so has $N_0 + 4$ outcomes, each associated with a probability.

For FC it is possible to calculate the entropy rate directly under certain assumptions. If we treat the position of the random walker as effectively in equilibrium over the network, meaning $r_W \gg r_N$, we have that $p_i \approx 1/V(t)$. The trajectory of a random walker on a network that grows under FC can be thought of as sampling from a fair $(N(t) + N_0)$-sided die. The entropy rate is therefore

$$\lim_{N\to\infty} \frac{1}{N} \log \frac{N!}{(N_0 - 1)!}, \qquad (5)$$

which diverges as $N \to \infty$. A growing fair die can be seen as the 'most' divergent entropy rate for the network growth mechanisms we present here. Fig. 4 shows that, for WING, finite entropy rates appear to exist for all values of r_W and are an increasing function of r_W. In contrast, the entropy rates for BA and FC are divergent.

We next aim to determine whether the distribution described by (1) for WING converges on a distribution with finite entropy in the limit $V \to \infty$. If so, the entropy rate associated with the trajectories of the random walker will be well-defined and the trajectories compressible. To demonstrate that $l(i, V)$ has finite entropy as $V \to \infty$ in the limit we proceed in two parts. First, we demonstrate that the probability of being at a node of a given age when the next growth event occurs is bounded below as $V \to \infty$. Second, we argue that the tail of $l(i, V)$ decays appropriately.

To approach the first part, we recast $l(i, V)$ in terms of node age $a = V - i + 1$, as in Fig. 3, and write $\rho(a)$

for $l(a, V)$ as $V \to \infty$. The claim is that

$$\rho(a) > \alpha_a, \ \forall \ a \text{ as } V \to \infty, \tag{6}$$

where α_a is a constant dependent on the age of the node and the parameters of the model. In this notation, $a = 1$ is the last node that was added to the network, $a = 2$ is the second to last node added to the network, and so on. Expression (6) states that the probability of being at a node of age a is bounded below in the limit of large network size.

We show first that this is true, in particular, for the probability $\rho(1)$ of being at the newest node in the network when the next growth event occurs. Let $\langle k_W \rangle$ be the expectation of the degree of the node that the walker is at just after a growth event. Note that $\langle k_W \rangle$ is necessarily distinct from the global degree average, $\langle k \rangle$, which in this model is always 2 [10]. The next event in the system is either a step by the walker or another growth event. The former occurs with probability $m = r_W/(r_W + r_N)$; the latter with probability $g = r_N/(r_W + r_N)$. If a growth event occurs next, the walker is one step away from the new node (of age 1) created in the event. If the subsequent event is a step by the walker, the walker can choose uniformly among, on average, $\langle k_W \rangle + 1$ available neighbors, one of which is the node just attached. Thus, the probability that the walker ends up at the node of age 1 is at least the probability of the event sequence 'growth and one step in the right direction':

$$\rho(1) > g\, m \frac{1}{\langle k_W \rangle + 1}. \tag{7}$$

It is at least this probability, because there are many, more circuitous, paths to reach the new node before it ages. If $\langle k_W \rangle$ is stationary in the limit, the bound (7) is independent of network size and thus of time. Analogous reasoning leads to

$$\rho(a) > g^{a-1}\, g\, m \frac{1}{\langle k_W \rangle + a}. \tag{8}$$

The claim (6) is shown if we can ascertain the relevant properties of $\langle k_W \rangle$. For example, $\langle k_W \rangle$ and $\langle k_W^2 \rangle$ should be finite and the local degree distribution monotonic, such that $\langle k_W \rangle$ is a meaningful proxy of local network structure. In prior work, we showed that these properties indeed hold [10].

Implicit in the above is that all higher order probabilities can be bounded below in a similar manner. For instance, if we define $\rho(a, b)$ as the joint probability that a growth event occurs at a node of age b followed by a growth event at a node of age a, then for $a \leq b$

$$\rho(a, b) > \rho(b - a + 1) g^{a-1}\, g\, m \frac{1}{\langle k_W \rangle + a}. \tag{9}$$

The right-hand-side of (9) describes a growth event at a node of age $b - a + 1$, followed by $a - 1$ growth events at this node. The node the walker is situated on has now age b and langle $\langle k_W \rangle + a - 1$ neighbors, one of which has age $a - 1$. A growth event occurs next, followed by a movement event to the node of age a, which is the last node added. Likewise, for $a > b$:

$$\rho(a, b) > \rho(1) g^{a-2} m \frac{1}{\langle k_W \rangle + a - 1} g\, m\, g. \tag{10}$$

It follows from these bounds that conditional probabilities, such as $\rho(a|b)$, defined as a growth event at the node of age a conditioned on the preceding growth event having occurred at the node of age b, are also bounded below, since $\rho(a|b) = \rho(a, b)/\rho(b)$ and the ratio is bounded.

FC is an example of a growth mechanism for which $\rho(a)$ is not bounded below in the limit. Although the new node is always adjacent to the node at which the walker is situated, the probability of moving to this new node (or any other neighboring node), given a movement event, is $1/(V - 1)$, which is not bounded below in the limit $V \to \infty$. Similarly, for BA network growth, the new node is increasingly less likely to be adjacent to the walker as $V \to \infty$, and so the distance from the walker to the new node is a function of network size.

Continuing with this reasoning, we can calculate the expected degree $\langle k_i \rangle$ of a node given its age in the limit $V \to \infty$. Each node introduced to the network is of degree $k = 1$, and has a probability $\rho(1)$ of the walker being situated on it at the next growth event and so having its degree increased by one; or a probability $\rho(2)$ of the walker being situated on it at the following growth event and so having its degree increased by one; and so on. Therefore,

$$\langle k_i \rangle = 1 + \sum_{j=1}^{\infty} 1 \cdot \rho(j) = 2. \tag{11}$$

The independence of $\langle k_i \rangle$ from age was suggested already by Fig. 1.

Finally, we need to argue that the tail of the probability distribution $\rho(a)$ decays in such a way that the entropy is finite as $V \to \infty$. After a growth event has occurred at a node of undefined age $\hat{a}$ (and no movement event has occurred since), the random walker must be situated on a node that shares an edge with the newest node in the network. Hence, the expected distance between the node $\hat{a}$ at which the walker is located and a node of age a is $d(\hat{a}, a; V) = d(1, a; V) - 1 \approx d(1, a; V)$, which is independent of $\hat{a}$. Moreover, since $\rho(a|1)$ is bounded below as $V \to \infty$ (for a given a), the expected distance $d(\hat{a}, a; V)$ must be bounded above as $V \to \infty$. Hence, barring oscillations in the expected distances between nodes we can write as $V \to \infty$: $d(\hat{a}, a; V) \to d(\hat{a}, a) \to d(1, a) - 1$, independent of network size V. In the Supplemental Material [15] we numerically demonstrate that the expected distance between two nodes appears to be a linear function of the difference in their age (independent of V). If we assume that the expected distance between node 1 and node a grows linearly with a, we can recast the problem

as diffusion of a random walker in one dimension. Therefore, the probability the next growth event occurs at a node of age a is bounded above by $O(e^{-a^2})$ as $V \to \infty$, and so would admit a finite entropy. Alternatively, if the expected distance between nodes in the network does not increase as a linear function of age difference (but logarithmically, for instance), it is possible that despite lower bounds, $\rho(a)$ would not admit a finite entropy as $V \to \infty$.

It is well understood that compressibility (in practice) takes advantage of non-uniformities in the probability distribution being sampled from [16]. We have argued that WING generates a nonuniform distribution of the walker's position that has a finite entropy as $V \to \infty$. This means WING generates a typical set of random walker trajectories with the following property

$$e^{-V(H(\mathcal{X})+\epsilon)} \leq p(x_1, x_2, \ldots, x_V) \leq e^{-V(H(\mathcal{X})-\epsilon)}, \quad (12)$$

where $H(\mathcal{X})$ is the entropy rate associated with the walker's position for fixed values of $0 < r_W < \infty$ and $0 < r_N < \infty$.

In conclusion, we have shown that growth, typically associated with increasing the number of states accessible to a process, can also function to constrain the likely outcomes of a process. The effects of state space growth in statistical mechanics have long been of interest, such as the increase in entropy associated with an expanding gas. The cost for the compressibility of WING trajectories is that the mechanism must know the location of the walker. This is not unlike using informed manipulation to control uncertainty in variations of Maxwell's demon [17, 18].

It is still to be determined whether the compressibility of random walker trajectories is a common property of network growth mechanisms that couple network growth and the position of a random walker (or another process situated on the network). However, given the simple set of conditions provided here for compressibility it seems reasonable to assume a range of network growth models may exhibit compressibility. It is also important to highlight the effect different types of growth may have on compressibility. In this work we have employed linear growth with our network growth models, but had we employed exponential growth we would not have observed the compressibility of random walker trajectories we did with WING. This is because the effective network growth rate is $r_N V$, and the ratio $r_W/(r_N V)$ tends to zero as $V \to \infty$ [10]. As a result, the local environment of the walker becomes increasingly "star-like", and so differs from the situation in which $r_W = 0$, when random walker trajectories are trivially compressible.

Finally, the Shannon entropy is the value of the Rényi entropy $H_\alpha(X) = 1/(1-\alpha)\log\left(\sum_{i=1}^n p_i^\alpha\right)$ as $\alpha \to 1$. Other limiting values of the Rényi entropy, such as when $\alpha = 1/2$, have been the subject of research interest. $H_{1/2}(X) = 2\log\left(\sum_{i=1}^n p_i^{1/2}\right)$ has been shown to bear relation, in the limit $n \to \infty$, to the average guesswork needed for identifying the value of a random variable [19, 20]. Following our treatment of entropy rates in WING, $H_{1/2}(X)$ would converge. This means that the expected number of guesses to find the walker (using an optimal guessing strategy) would remain finite (and bounded) as $V \to \infty$. Being able to efficiently find the walker in the network is important for the practical feasibility of WING and, more generally, the feasibility of any network growth mechanism whereby a process on the network must be analyzed in some manner before the growth event can occur. Alternatively, network growth algorithms may exist in which random walker trajectories are compressible but not predictable, and so the feasibility of these algorithms would depend on whether the growth mechanism was local to the network or required a global analysis before being completed.

I. ACKNOWLEDGEMENTS

RJHR would like to acknowledge Ioana Cristescu, Muriel Médard and Ken Duffy for helpful discussions related to the work presented here.

[1] R. McLennan, L. Dyson, K. W. Prather, J. A. Morrison, R. E. Baker, P. K. Maini, and P. M. Kulesa, Development **139**, 2935 (2012).
[2] R. L. Mort, R. J. H. Ross, K. J. Hainey, O. Harrison, M. A. Keighren, G. Landini, R. E. Baker, K. J. Painter, I. J. Jackson, and C. A. Yates, Nature Communications **7** (2016).
[3] R. J. H. Ross, R. E. Baker, and C. Yates, Physical Review E **94**, 012408 (2016).
[4] R. J. H. Ross, C. A. Yates, and R. E. Baker, Physical Review E **95**, 032416 (2017).
[5] M. Newman, *Networks: an introduction* (Oxford University Press, 2010).
[6] M. F. Bear, B. W. Connors, and M. A. Paradiso, *Neuroscience: exploring the brain*, 3rd ed. (Lippincott Williams and Wilkins, Philadelphia, 2007).
[7] T. M. Cover and J. A. Thomas, *Elements of information theory* (John Wiley & Sons, 2012).
[8] J. Saramäki and K. Kaski, Physica A: Statistical Mechanics and its Applications **341**, 80 (2004).
[9] T. S. Evans and J. P. Saramäki, Physical Review E **72**, 026138 (2005).
[10] R. J. H. Ross, C. Strandkvist, and W. Fontana, arxiv (2018).
[11] D. T. Gillespie, Journal of Physical Chemistry **81**, 2340 (1977).

[12] P. L. Krapivsky, S. Redner, and F. Leyvraz, Physical Review Letters **85**, 4629 (2000).
[13] S. N. Dorogovtsev, J. F. F. Mendes, and A. N. Samukhin, Physical Review Letters **85**, 4633 (2000).
[14] C. Cannings and J. Jordan, Electronic Communications in Probability **18** (2013).
[15] See Supplemental Material at http://... for details of analytical calculations and further simulation results.
[16] C. Shannon, Bell System Technical Journal **27**, 379 (1948).
[17] L. Szilard, Zeitschrift für Physik **53**, 840 (1929).
[18] R. Landauer, IBM Journal of Research and Development **5**, 183 (1961).
[19] J. L. Massey, in *Information Theory, 1994. Proceedings., 1994 IEEE International Symposium on* (IEEE, 1994) p. 204.
[20] E. Arikan, IEEE Transactions on Information Theory **42**, 99 (1996).

Compressibility of random walker trajectories on growing networks Supplemental Material

A. LOCAL AND GLOBAL DEGREE DISTRIBUTION OF WING

Let $p_W(k)$ denote the probability that the walker is situated at a node of degree k when a growth event occurs. To obtain $p_W(k)$ numerically we record the trace t_r of degrees seen by the walker in a simulation r, collect the frequency with which the degree is k at growth event g across replicate traces t_r (r indexing the replicate) each comprising N growth events, and average over g. Denoting the degree the walker observes at event g of trace t_r by $t_{r,g}$, we have

$$p_W(k,g) = \frac{1}{R}\sum_{r=1}^{R}\delta(k - t_{r,g})$$
$$p_W(k) = \frac{1}{V}\sum_{g=1}^{V} p_W(k,g)$$

where $\delta(x) = 1$ if $x = 0$ and $\delta(x) = 0$ otherwise. The global degree distribution $p(k)$ is computed likewise, but instead of observing a single node at growth event g, we observe all nodes in the network.

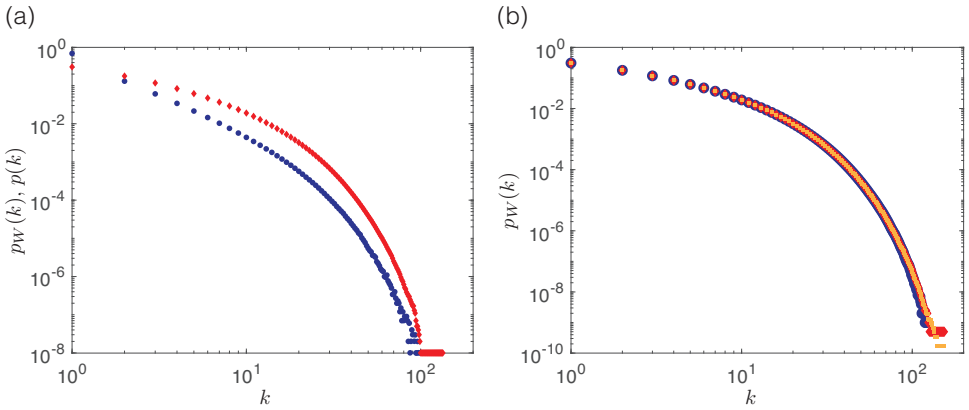

FIG. SF1. Local and global degree distribution. Panel (a): The global degree distribution $p(k)$ (blue disks) is compared with the degree distribution seen by the walker $p_W(k)$ (red diamonds) after $N = 10,000$ growth events. $r_W = 5$, $r_N = 1$. Panel (b): Convergence of $p_W(k)$ to a stationary distribution is rapid. $p_W(k)$ is depicted for different growth extents: $N = 10,000$ (blue filled circles), $N = 20,000$ (red diamonds), and $N = 100,000$ (orange squares).

B. THE AVERAGE DISTANCE BETWEEN TWO NODES AS A FUNCTION OF AGE

The average distance between two nodes in networks with WING is a linear function in the difference in their ages and does not depend on the size of the network. The distance between nodes for networks grown with WING is maximized between $r_W = 0.5$ and $r_W = 1$. Figure SF2 also evidences that the age of a node and its degree do not positively correlate in WING.

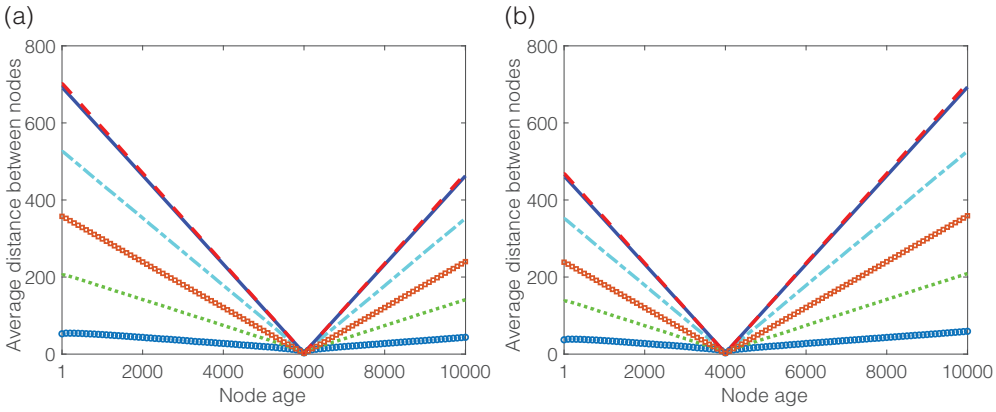

FIG. SF2. Distance between nodes as a function of age. Panel (a): The average distance between a node of age 4000 and all other nodes in a network generated with WING is shown as a function of their age difference for different values of walker motility. $r_W = 10$ (blue circles), $r_W = 5$ (green dashed), $r_W = 2$ (blue dot-dashed), $r_W = 1$ (blue solid), $r_W = 0.5$ (red dashed) and $r_W = 0.1$ (red squares). Panel (b): As in panel (a), but for node 6000. In both panels $N = 10,000$.